Toward the Development of Partially Biodegradable and Injectable Thermoresponsive Hydrogels for Potential Biomedical Applications

De-Qun Wu,[†] Fen Qiu,[†] Tao Wang,[‡] Xue-Jun Jiang,[‡] Xian-Zheng Zhang,*[,†] and Ren-Xi Zhuo*[,†]

Key Laboratory of Biomedical Polymers of Ministry of Education, Department of Chemistry, Wuhan University, Wuhan 430072, People's Republic of China, and Department of Cardiology, Renmin Hospital of Wuhan University, Wuhan 430060, People's Republic of China

ABSTRACT A series of hydrogels containing a biodegradable dextran (Dex) chain grafted with a hydrophobic poly(ϵ-caprolactone)−2-hydroxylethyl methacrylate (PCL−HEMA) chain and a thermoresponsive poly(*N*-isopropylacrylamide) (PNIPAAm) chain were synthesized. The molecular weight of PCL−HEMA was determined by gel permeation chromatography, and the inner morphology of the hydrogel was observed by scanning electron microscopy. The release profiles from the hydrogels were investigated using bovine serum albumen as a model drug. It was found that the release behavior could be adjusted by varying the composition of the hydrogel. In vitro cytotoxicity studies of the hydrogels showed that the copolymer Dex−PCL−HEMA/PNIPAAm exhibited low cytotoxicity. The in vivo degradation and histological studies demonstrated that the hydrogels had good biocompatibility and were promising for use as an injectable polymeric scaffold for tissue engineering applications.

KEYWORDS: injectable biodegradable hydrogel • thermoresponsive • histology study • biocompatibility

INTRODUCTION

Polymeric hydrogels are cross-linked polymer networks that can absorb a large amount of water, making them more similar to soft tissues (1, 2). In addition, because hydrogels are porous, the exchange of oxygen, nutrients, and other water-soluble metabolites can easily take place inside the hydrogel networks. Among the hydrogels, intelligent hydrogels are capable of changing their shape, structure, or volume when exposed to external stimuli, for example, pH (3−5), temperature (6−8), antigen (9), electric field (10), and light (11).

In recent years, an increasing number of injectable hydrogels have been reported for multifarious biomedical applications, such as cell encapsulation (12−14), drug delivery (15−19), and tissue engineering (20, 21). Injectable materials have advantages in clinic applications because of their fluidity, which enables the materials to be introduced into the site-specific organ, tissue, or body cavity with improved patient applicability and comfort (14, 22−24). Among those stimuli-sensitive hydrogels, poly(*N*-isopropylacrylamide) (PNIPAAm) hydrogel shows a lower critical solution temperature (LCST) at around 33 °C in aqueous solution and changes volume and shape abruptly and thermoreversibly (25). This property was used in the attachment/detachment of cultured cells (26), drug release, and immobilization of enzymes. On the basis of this concept, several injectable hydrogels using PNIPAAm were reported (20). For example, Stile et al. fabricated PNIPAAm and poly(NIPAAm-*co*-acrylic acid) hydrogels for supporting bovine articular chondrocyte viability for at least 28 days in vitro culture, and cartilage-like tissue formed in the matrixes. However, because of their nonbiodegradability, PNIPAAm hydrogels were restricted for some specific biomedical applications (27). Recently, Liu and co-workers (28) reported the thermosensitive F127 hydrogel for controlled release of peptide and protein drugs after subcutaneous injection. Although those injectable hydrogels had the property of biocompatibility, the absence of biodegradability of the hydrogel might limit their wide application in vivo. It is obvious that there is considerable scope for the development of injectable hydrogels with both biocompatibility and biodegradability.

Dextran (Dex) composed of α-1,6-D-glucopyranose residues is a naturally biodegradable polymer and is liable to enzymatic digestion in the human body. Because of its biocompatible and biodegradable properties, Dex and its derivatives have been exploited extensively in the fields of biomedical, biotechnological, and pharmaceutical applications (29−32). Poly(ϵ-caprolactone) (PCL), a well-known biodegradable aliphatic polyester with good biocompatibility and flexibility, has been widely explored as a scaffold in tissue engineering (33, 34) and a matrix in drug controlled

* To whom correspondence should be addressed. Tel.: + 86-27-6875 4061. Fax: + 86-27-6875 4509. E-mail: xz-zhang@whu.edu.cn (X.-Z.Z.), bmp@whu.edu.cn (R.-X.Z.).

Received for review September 09, 2008 and accepted September 17, 2008

[†] Wuhan University.

[‡] Renmin Hospital of Wuhan University.

DOI: 10.1021/am8000456

Scheme 1. Schematic Illustration of the Synthesis of Dex−PCL−HEMA Macromonomer

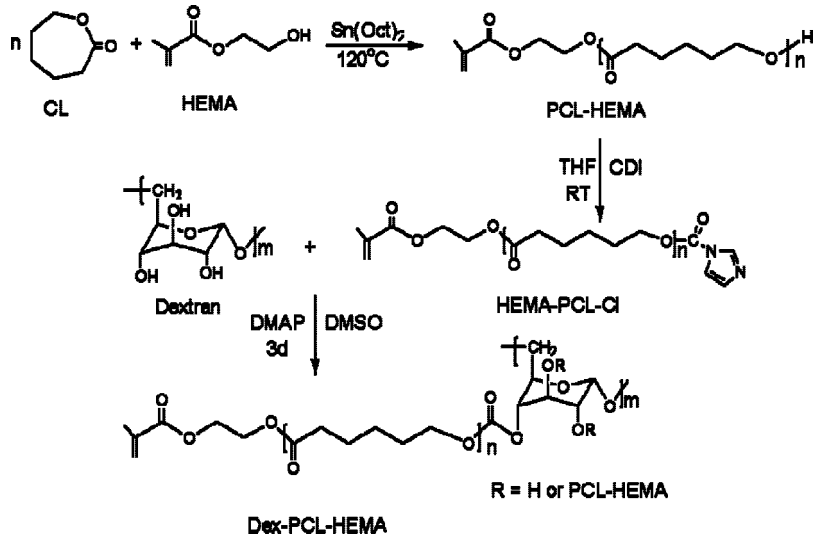

release (35). The mechanism of biodegradation through hydrolysis of the ester linkage and the normal intermediates of cell metabolism as its decomposition products is the main characteristic of PCL (36).

In this study, a series of novel biodegradable hydrogels were synthesized by the introduction of PCL-grafted polysaccharide chains into the PNIPAAm network. Because of the existence of the amphiphilic structure of the PCL-grafted Dex chains and the thermoresponsive PNIPAAm chains, the resulting hydrogels can shift from sol to gel within 1 min and the reversible course occurs in the same time. In vitro enzymatic biodegradability of the thermoresponsive copolymer and drug release was also investigated. Moreover, in vivo experiments of the hydrogels were performed.

MATERIALS AND METHODS

Dextran (Dex) was obtained from *Leuconostoc mesenteroides* (M_w = 60 000−90 000 g/mol), and *N*-isopropylacrylamide (NIPAAm), *N*,*N*′-carbonyldiimidazole (CDI), and ϵ-caprolactone (CL) were purchased from Sigma and used as received. 2-Hydroxylethyl methacrylate (HEMA), tetrahydrofuran (THF), and dimethyl sulfoxide (DMSO) were obtained from Shanghai Chemical Reagent Co., China, and used after distillation under reduced pressure. Ammonium persulfate (APS), *N*′,*N*′,*N*′,*N*′-tetramethylethylenediamine (TEMED), bovine serum albumin (BSA; M_w = 67 000 g/mol), sodium azide, 4-(*N*,*N*-dimethylamino)pyridine (DMAP), and 2,6-di-*tert*-butyl-4-methylphenol were obtained from Shanghai Chemical Reagent Co., China, and used as received. A total of 29 male adult Wistar rats with weights of 220−260 g were bought from the laboratory animal center, Tongji Medical Institute, Huazhong University of Science and Technology, China.

Synthesis of Dex−PCL−HEMA Macromonomer. Dex−PCL−HEMA was synthesized as follows: CL (6.84 g, 0.06 mol) and HEMA (0.039 g, 0.003 mol) were reacted in the presence of catalyst $SnOct_2$ (0.01341 g, 1.0 mol % with respect to HEMA) and 2,6-di-*tert*-butyl-4-methylphenol (0.067 g) under vigorous stirring in a glass ampule under vacuum at 120 °C for 3 h. The HEMA−PCL product was collected by dissolution of the cooled reaction mixture in methylene dichloride, precipitation at least twice in a 10-fold ice-cold methanol, and filtration under reduced pressure. Precipitation in methanol was to remove residual HEMA in the product. The collected solid was dried under vacuum overnight. The yield was 70 %. Next, HEMA−PCL (2.105 g, 0.0005 mol) and CDI (0.162 g, 0.001 mol) were dissolved in THF (50 mL) in a nitrogen atmosphere with vigorous stirring for 16 h. The resulting HEMA−PCL−imidazolyl carbamate (CI) was obtained by solvent evaporation under reduced pressure. Finally, Dex (9.72 g, 0.06 mol of glucopyranose residues) was dissolved in 60 mL of DMSO in a nitrogen atmosphere. After dissolution of DMAP (0.15 g), HEMA−PCL−CI was added, and the mixture was stirred at room temperature (25 °C) for 4 days. The Dex−PCL−HEMA product was obtained by precipitation of the reaction mixture in a large excess volume of chilled 2-propanol, washed several times with 2-propanol, and dried in a vacuum for 24 h. The schematic illustration of the synthesis of Dex−PCL−HEMA is shown in Scheme 1.

Table 1. Preparation of the Dex−PCL−HEMA/PNIPAAm Hydrogels

	sample code[a]			
composition	DN1	DN2	DN3	DN4
Dex−PCL−HEMA (mg)	10	20	30	40
NIPAAm (mg)	190	180	170	160
APS (mg)	10	10	10	10
TEMED (μL)	10	10	10	10
H_2O (mL)	1.5	1.5	1.5	1.5

[a] All reactions were performed at room temperature for 24 h.

Synthesis of Thermoresponsive Hydrogels. NIPAAm monomer and Dex−PCL−HEMA were dissolved in a phosphate-buffered saline (PBS) solvent (pH 7.4) at different weight ratios to form a monomer solution, and the radical polymerization of NIPAAm hydrogels was carried out in glass vessels at room temperature for 24 h, using APS (5.0 wt % based on Dex−PCL−HEMA and NIPAAm) and TEMED as the redox initiator and accelerator, respectively. The feed compositions of the monomers and other reactants are listed in Table 1, and the resulting hydrogels were designated as DN hydrogels. Finally, the DN hydrogels were transferred to the dialysis tube (molecular weight cutoff: 8000−12 000 g/mol) for dialysis against a PBS solution (pH 7.4) for 2 days, and the PBS solution was refreshed every 12 h. After dialysis was finished, the hydrogels were moved to different glass vessels and cooled in a refrigerator at −20 °C overnight, followed by freeze drying. The freeze-dried hydrogels (80 mg) were dissolved in a PBS solution (pH 7.4, 1 mL) to form injectable hydrogels.

^{1}H NMR. The ^{1}H NMR spectra of Dex, PCL−HEMA, and Dex−PCL−HEMA macromonomer were recorded on a Mercury VX-300 spectrometer at 300 MHz (Varian, Palo Alto, CA) by using $CDCl_3$ or DMSO-d_6 as the solvent and tetramethylsilane as the internal standard. For PCL−HEMA, deuterated chloroform ($CDCl_3$; 99.9%, Aldrich) was used as the solvent and the chloroform-d_1 resonance was set at 7.27 ppm. For Dex and Dex−PCL−HEMA macromonomer, DMSO-d_6 (99.9%, Aldrich) was used as the solvent and the central DMSO line was set at 2.50 ppm.

Fourier Transform Infrared (FTIR) Spectroscopy. FTIR spectra were recorded on a spectrometer (an Avatar 360 spectrometer) to characterize the chemical structures of Dex, Dex−PCL−HEMA, and DN2 hydrogel by studying their IR absorption bands, which match their natural vibrational modes. The samples were ground into pieces and compressed onto the KBr crystal, and FTIR spectra were recorded in the wavenumber range of 600−4000 cm^{-1}.

Gel Permeation Chromatography (GPC). The molecular weights of the copolymers were determined by a GPC system equipped with a Waters 2690D separation module and a Waters 2410 refractive index detector (THF was used as the eluent). The molecular weight was calculated by Waters millennium module software on the basis of a universal calibration curve produced by polystyrene standards with narrow molecular weight distribution.

LCST Determination. The freeze-dried hydrogels were dissolved in PBS solutions (pH 7.4) with different volumes at room temperature to determine the absorbance of the solutions. Optical absorbance of the solutions was measured by a Lambda Bio40 UV−vis spectrometer (Perkin-Elmer) using UV absorbance at 500 nm. Transmittance measurements and determination of the LCST at various temperatures were measured. Prior to measurements, the sample cell was thermostated in a refrigerated circulator bath at different temperatures from 26 to 36 °C. The LCST values of the copolymer solutions were determined at the temperature showing a half increase of the total absorbance.

Interior Morphology of the Hydrogels. All of the Dex−PCL−HEMA/PNIPAAm hydrogels were mixed with a 5 wt % mannitol solution and transferred to an 8-mL vial. After incubation in 37 °C water for 3 h, the hydrogels were frozen quickly in liquid nitrogen and freed-dried in a Virtis Freeze Drier under vacuum at −51 °C for 2 days until all of the water was sublimed. The interior morphology of the hydrogels was observed by scanning electron microscopy (SEM).

Rheological Characterization of the Hydrogels. The dynamic rheology was measured on an ARES-RFS III rheometer (TA Instruments, New Castle, DE). Double concentric cylinder geometry with a gap of 2 mm was used to measure steady viscoelastic parameters as functions of the shear rate. Temperature control was established by connection with a julabo FS18 cooling/heating bath kept within 0.2 °C. To measure temperature-dependent gelation of the hydrogel, temperature sweeps were performed from 18 to 48 °C with a heating rate of 1 °C/min. The data was collected at a frequency of 1 Hz and a controlled strain of 1%. The strain was controlled as low as possible to minimize the influence of disruption of the hydrogel network in order to perform in the linear viscoelastic range (37, 38). The sol-to-gel transition temperature was defined as the temperature at which the storage modulus (G') increased rapidly and reached a plateau.

Sol−Gel Transition and Injectability Test of the Hydrogels. The sol−gel phase transition temperature of the Dex−PCL−HEMA/PNIPAAm copolymer in a PBS solution (pH 7.4, 8.0 wt %) was recorded using the inverting test method with a 6-mL glass vial, which was equilibrated at 25−37 °C in a thermostated water, "inversion tube method" (39, 40). Briefly, after equilibration in a water bath for 30 min, the vial was heated slowly to the desired temperature with 2 °C increments in the water bath. The vial was held constant to equilibrate at each temperature for 10 min and then laid down horizontally for 1 min. The gel state was determined when no fluidity was visually observed within 1 min.

In Vitro Enzymatic Diodegradation of the Hydrogels. The in vitro biodegradation of the thermoresponsive hydrogels was investigated by measuring the weight changes at 37 °C. Several parallel samples were put into 50 mL of a PBS solution (pH 7.4, $I = 0.2$ M) in centrifugal test tubes with a 0.2 mg/mL of lipase from *Pseudomonas cepacia* and 0.2 mg/mL of sodium azide (retarding bacterial growth) solution. The centrifugal test tubes were put into a shaking bed and agitated at 50 cycles/min at 37 °C. The enzyme and sodium azide solutions were refreshed every 3 days. The biodegraded samples were taken out at the programmed time and dried under vacuum for 2 days to determine the dry weight of the hydrogels. The weight loss (%) was calculated as weight loss (%) $= (W_0 - W_t)/W_0 \times 100$, where W_t is the dry weight of the programmed time and W_0 is the initial dry weight of the hydrogels before biodegradation.

In Vitro Release of BSA from the Hydrogels. The general protocol for the in vitro drug release study is exemplified by the following procedure. A total of 20 mg of BSA ($M_n = 67\,000$ g/mol) was dissolved in 1000 mg of a hydrogel PBS solution (8.0 wt % hydrogel), which was added into a 50-mL cuvette. The solution was thoroughly mixed and then incubated in a 37 °C water bath overnight, allowing the mixture to form a viscous hydrogel. Then 20 mL of a 37 °C PBS solution was added to the cuvette and incubated in a 37 °C water bath. At predetermined times of the in vitro release experiment, 4-mL aliquots of the buffer medium were removed from the cuvette, the concentration of the BSA in the aliquot was measured by using a UV absorbance (Lambda Bio40 UV−vis spectrometer, Perkin-Elmer) at 280 nm, and a BSA standard calibration curve was generated at each time using a nonloaded hydrogel solution in order to correct the intrinsic absorbance. A 4-mL fresh buffer solution prewarmed at 37 °C was added back to the cuvette to maintain the same total solution volume. The DN2 without loading BSA was used as the control. The cumulative BSA release (%) was calculated as cumulative release (%) $= M_t/M_0 \times 100$, where M_t is the amount of BSA released from the hydrogels at time t and M_0 is the weight difference of the initial BSA loaded in the hydrogels and the remaining BSA in the buffer after loading. All of the release experiments were conducted in triplicate.

In Vitro Cytotoxicity of the Thermoresponsive Hydrogel. In vitro cytotoxicity test was carried out as follows: 200 μL of a human vascular endothelial cell line, ECV304 in DMEM with a concentration of 1.25×10^4 cells/mL, was added to each well in a 96-well plate. The number of ECV304 in each well is 2.5×10^3. After incubation for 24 h in an incubator (37 °C, 5% CO_2), the culture medium was replaced by 200 μL of DMEM containing the Dex−PCL−HEMA/PNIPAAm copolymer (8.0 wt % hydrogel) with particular concentrations, and the mixture was further incubated for 48 h. Then, DMEM with the polymer was replaced by fresh DMEM, and 20 μL of a MTT solution (5 mg/mL) was added to the fibroblasts. After incubation for 4 h, 200 μL of DMSO was added and shaken at room temperature. The optical density (OD) was measured at 570 nm with a Microplate Reader model 550 (Bio-Rad Laboratories, Herculaes, CA). The viable rate was calculated by the following equation: viable rate $= OD_{treated}/OD_{control}$, where $OD_{control}$ was obtained in the absence of polymer and $OD_{treated}$ was obtained in the presence of polymer.

Sterilization of the Hydrogels. Before in vivo study, the DN2 hydrogel was autoclaved at 120 °C for 20 min and then stored at 4 °C for 12 h (41).

Subcutaneous and Intramuscular Injection of the Hydrogels into Rats. The rats were acclimated for 1 week

before being used, and the DN2 hydrogel was used in the experiments. Rats were permitted access to standard food freely (laboratory animal center, Renmin Hospital of Wuhan University, China) and tap water. All care and handling of the animals were performed with the approval of Institutional Authority for Laboratory Animal Care. A total of 29 rats were randomly divided into three groups: group 1 (9 rats) for injection of 0.5 mL of PBS subcutaneously (SC) beneath the dorsal skin between the scapulae and the same dose intramuscularly (IM) in the hind leg; group 2 (10 rats) for injection of 0.5 mL of hydrogel SC beneath the dorsal between the scapulae; group 3 (10 rats) for injection of 0.5 mL of hydrogel IM in the hind leg. Rats were anesthetized by pentobarbital before injection. Hydrogel and a PBS solution (pH 7.4, ionic strength = 0.2 M) were transferred respectively into a 1-mL syringe mounted with a 18-G needle and injected into each rat. The needle was held in place for 1 or 2 s before withdrawal to prevent the hydrogel from outflowing from the injection site.

Regional inflammation, leg movement, and food intake were observed after injection every day. The transverse diameter of the hydrogel was measured in group 2 every day.

Blood (1.2 mL) was obtained from each rat 1 week after the hydrogel injection: 0.2 mL for blood count and the remaining 1 mL to measure the concentration of the biochemical indicators aspartate aminotransferase (AST), alanine aminotransferase (ALT), creatinine (Cr), blood urea nitrogen (BUN), and blood glucose. All of the indicators were measured by a Beckman automatic biochemistry analyzer in the Department of Clinical Laboratory, Renmin Hospital of Wuhan University, China.

Implants with surrounding tissues were obtained, then frozen, and dissected by a Shandon −20 °C freezing microtome immediately. Serial sections of 8 μm were stained with hematoxylin, erythrosin, and safran (HES). Photomicrographs of internal sections of each sample were taken with a Zeiss Axioskop light microscope and a color video camera.

All of the rats were sacrificed with overdose pentobarbital injection after the experiment.

Statistical Analysis. SPSS11.5 software was used for statistical analysis. Data analysis was performed by one-way analysis of variance (Anova) and the Tukey−Kramer procedure for post hoc comparison. $P < 0.05$ was considered statistically significant.

RESULTS AND DISCUSSION

Synthesis of Dex−PCL−HEMA Macromonomers and Hydrogels. ^{1}H NMR (Figure 1) confirmed the formation of PCL−HEMA and Dex−PCL−HEMA macromonomer. As shown in Figure 1B, the characteristic chemical shift peaks of HEMA residues were centered at 6.12 and 5.59 ppm (a; C**H**$_2$=C<) and 1.9 ppm [b; CH$_2$=C(C**H**$_3$)−] and the CL chain chemical shift peaks appeared at 2.15 ppm (e), 4.13 ppm (i), 1.21 ppm (g), 1.53 ppm (f), and 1.62 ppm (h). Parts B and C of Figure 1 also demonstrated characteristic peaks of the CL residues of both PCL−HEMA and Dex−PCL−HEMA at 1.21 ppm (e) and characteristic peaks of the glycopyranose backbone of Dex (Figure 1A) at 4.6 ppm for anomeric protons. The average length (DP$_{av}$) of the CL spacer graft in PCL−HEMA could be calculated from the ratio of the integral of **H**e to that of **H**a (Figure 1B). The degree of substitution (DS; amount of methacrylate groups per 100 DEX glucopyranose residues) of Dex−PCL−HEMA could be calculated by the ratio of the integral of the protons of vinyl ending groups to the integral of the anomeric protons (**H**a:**H**k). DP$_{av}$ and DS of this study were 24 and 3.13, respectively.

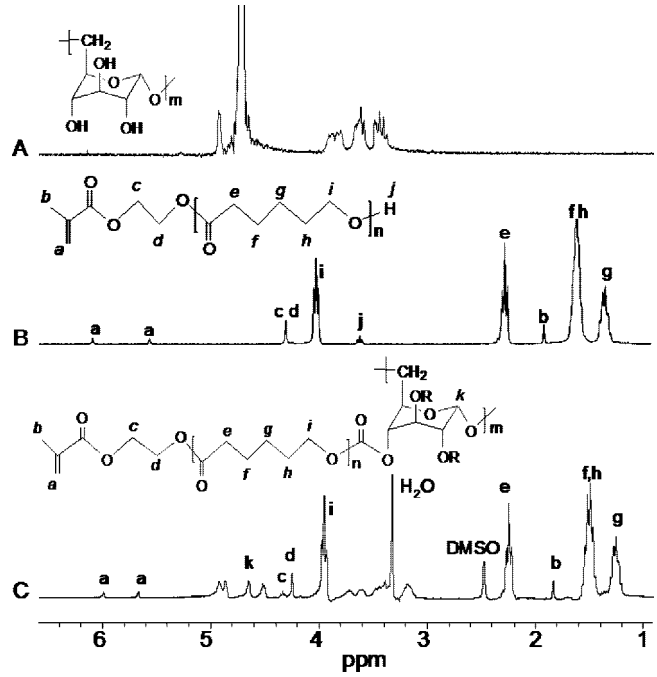

FIGURE 1. ^{1}H NMR spectra of Dex (A), PCL−HEMA (B), and Dex−PCL−HEMA (C).

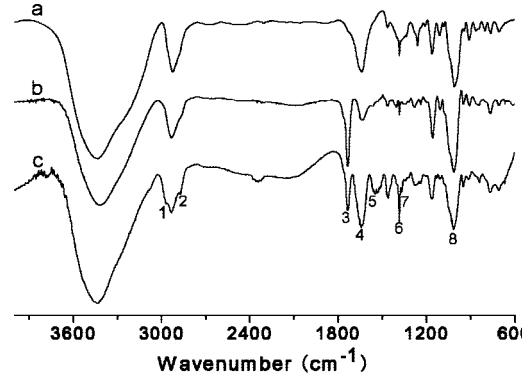

FIGURE 2. FTIR spectra of (a) Dex, (b) Dex−PCL−HEMA, and (c) Dex−PCL−HEMA/PNIPAAm hydrogel (DN2) (peaks 1 and 2, PCL chain vibrations; peak 3, C=O stretching; peak 4, amide I; peak 5, amide II; peaks 6 and 7, C−H bending of −CH(CH$_3$)$_2$; peak 8, C−OH stretching of Dex).

FTIR measurements were also used to verify the chemical structures of Dex, Dex−PCL−HEMA, and DN2 hydrogel. As shown in Figure 2, the characteristic bands of Dex−PCL−HEMA at 2944 and 2865 cm^{-1} (PCL chain vibration) and 1010 cm^{-1} (C−OH stretching from the Dex group) were observed in the IR spectra of the hydrogels. In addition, the characteristic band of Dex−PCL−HEMA was observed at 1740 cm^{-1} (C=O stretching from the PCL−HEMA group). The typical amide I and II bands at 1650 and 1540 cm^{-1} and divided bands of symmetric C−H bending from the −CH(CH$_3$)$_2$ group at 1385 and 1370 cm^{-1} from PNIPAAm of the hydrogels were also observed.

M_n calculated by ^{1}H NMR analysis was 3200, and the number- and weight-averaged molecular weights (M_n and M_w) of the polymers were determined by GPC. M_n, M_w, and PDI values for PCL−HEMA were 3420 g/mol, 4200 g/mol, and 1.2, respectively. These results were in agreement with

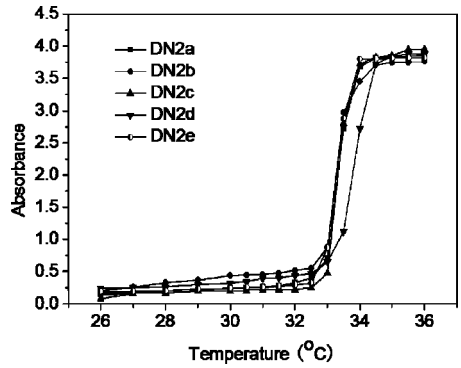

FIGURE 3. LCST determination of the DN2 hydrogels with different polymer concentrations (a, 0.5 wt %; b, 1.0 wt %; c, 1.5 wt %; d, 2.0 wt %; e, 2.5 wt %).

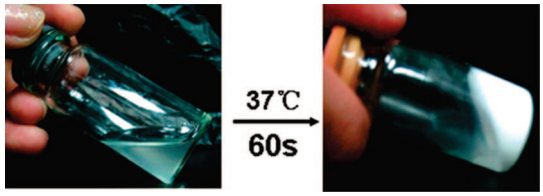

FIGURE 4. In situ gelation of the Dex−PCL−HEMA/PNIPAAm hydrogel with 8.0 wt % polymer concentration.

DP_{av} from ^1H NMR analysis and were considered as more evidence to the synthesis of PCL−HEMA.

LCST Determination. The effect of the temperature on the absorbance of visible light ($\lambda = 500$ nm) through the hydrogels with different polymer concentrations is shown in Figure 3. It is evident from Figure 3 that the hydrogel phase transition was very sharp, as shown in the graph. The LCST of the DN2 hydrogel was around 33.2 °C (32.8 ± 0.4 °C). The LCST of the PNIPAAm hydrogel is about 32 °C, as reported in the literature (42); the LCST of PNIPAAm can be changed by copolymerizing NIPAAm with other hydrophilic monomers (43, 44). Because of the addition of the hydrophilic monomer to the PNIPAAm-based hydrogel, the hydrophilic monomer prevents the dehydration of the polymer chains and expands the collapsed structure. As for the Dex−PCL−HEMA/PNIPAAm copolymer, the phase transition occurred at 33.2 °C because of the introduction of hydrophilic Dex−PCL−HEMA units. Although the CL spacer is hydrophobic in the Dex−PCL−HEMA segment, the hydrophilic Dex chain is longer than the hydrophobic PCL chain.

Sol−Gel Transition of the Hydrogels. Figure 4 demonstrates the sol−gel reversibility of the Dex−PCL−HEMA/PNIPAAm hydrogel in a PBS solution at pH 7.4. The sol−gel transition of the Dex−PCL−HEMA/PNIPAAm solutions occurred within 1 min with increased temperature. The gelation tests indicate that the gelation temperature is 33 °C, and well-stable hydrogels formed. The gel−sol transition also took a short time with decreased temperature. By studying the gelation of the Dex−PCL−HEMA/PNIPAAm solution with various polymer concentrations, we found that the higher the polymer concentration, the faster gelation happened, but there was no significant difference in the gelation time among the DN1, DN2, DN3, and DN4 hydrogels. When

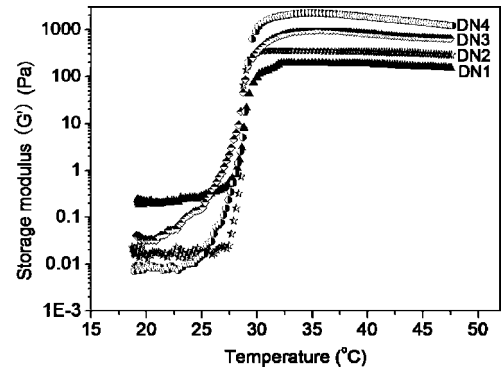

FIGURE 5. Storage modulus G' as a function of the temperature for DN series hydrogels in a PBS solution (pH 7.4) at a frequency of 1 Hz and 1% strain.

heated to 37 °C, which is above the LCST (33.2 °C) of DN hydrogels, the hydrophilicity/hydrophobicity balance of the PNIPAAm chains changed, leading to dehydration of the PNIPAAm chains. As shown in Figure 4, the hydrogel solution became opaque. It is important to point out that there is little water expelled from the hydrogel when heated to 37 °C, which indicated that there was much water still retained in the hydrogel after gelation at 37 °C and gelation took place in situ. The gel solution formed a stable hydrogel in situ via strong hydrophobic interactions above LCST. The advantage of the gel properties can be applied in the sustained delivery system for drugs and proteins as well as cells because acidic (below pH 6.5) or basic (above pH 8.5) conditions will induce the denaturation and toxicity of the protein and cell.

Rheological Characterization of the Hydrogels. Figure 5 shows the storage modulus G', which was described as a function of the temperature for the DN hydrogels in a PBS solution (pH 7.4) at a frequency of 1 Hz and 1% strain. As demonstrated in Figure 5, the storage modulus G' increases with an increase in the temperature, and at 29 °C, G' increased rapidly, which indicates gel formation (gel point). With the temperature increasing, G' reached a plateau at 32 °C. After that, G' remained constant, indicating that a stable gel was formed. Similar curves were obtained for all DN hydrogels. In the temperature range of 20−48 °C, the storage values of the hydrogels reach a stable plateau above 32 °C, which make the hydrogels reach a relative mechanical strength for a tissue scaffold. In the temperature range of 20−29 °C, the storage values of the hydrogels are less, which renders the hydrogels suitable for injection. The stable gelation temperature is almost equal to the LCST of the hydrogel. As shown in Figure 5, storage moduli of the hydrogels increase in the range from DN1 to DN4, which reveals that the mechanical strength of the hydrogel DN4 is the most, while DN1 is the least. This could be due to the cross-linking density of the hydrogel during the polymerization. With more cross-linker Dex−PCL−HEMA in the hydrogel, the mechanical strength of the hydrogel is stronger.

Interior Morphology of Dex−PCL−HEMA/PNIPAAm Hydrogels. The interior morphology of Dex−PCL−HEMA/PNIPAAm hydrogels is shown in Figure 6. The

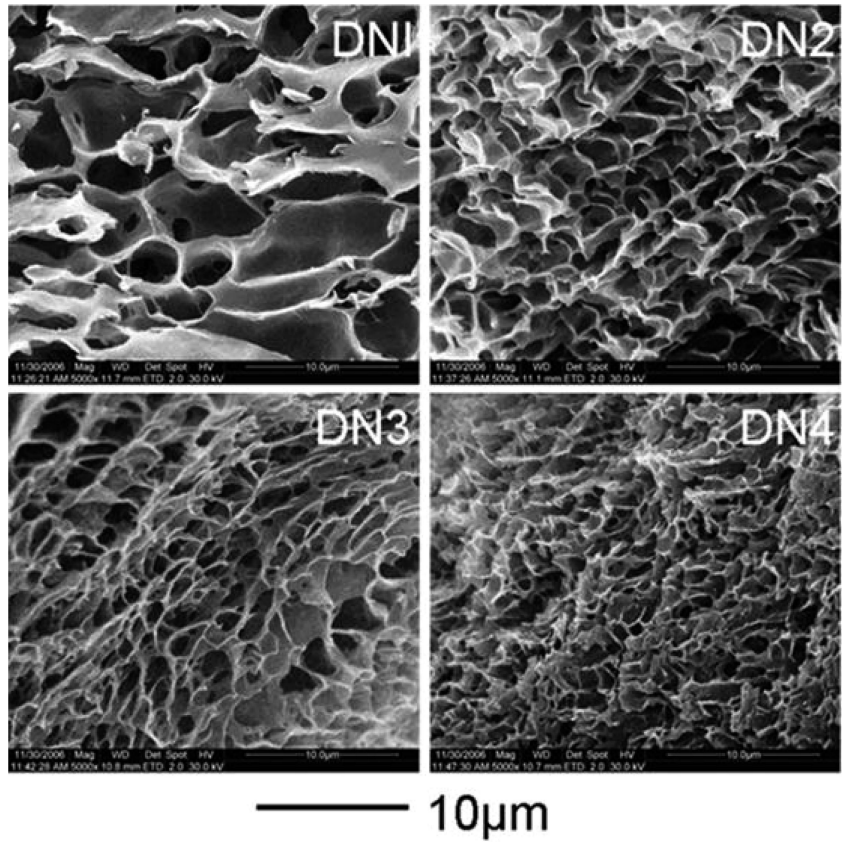

FIGURE 6. SEM micrographs of the Dex−PCL−HEMA/PNIPAAm hydrogels.

morphology of the hydrogels is a honeycomblike porous structure and is related to the composition ratio of Dex−PCL−HEMA to NIPAAm. The pore diameter of the hydrogels decreased with an increase in the ratio of Dex−PCL−HEMA/NIPAAm. The DN1 hydrogel has an average pore diameter of 8 μm, while the average pore diameter of DN4 is 2 μm. Among the DN series hydrogels, DN4 hydrogel has an average pore diameter of one-fourth that of DN1. The relationship between the pore diameter and the Dex−PCL−HEMA composition is due to an enhancement in the cross-linking density, which results from an increase in the Dex−PCL−HEMA composition because the cross-linkable group Dex−PCL−HEMA is located along the repeated glucose units of Dex backbone chains.

In Vitro Enzymatic Biodegradability of the Hydrogels. To investigate the degradation of the DN hydrogels, we used lipase from *P. cepacia*, which is known to catalyze the cleavage of ester bonds by transesterification (45). In the literature (46, 47), Dextranase was used to catalyze the degradation of Dex. As for the Dex−PCL−HEMA/PNIPAAm copolymer, lipase from *P. cepacia* was applied to catalyze the degradation of PCL from the Dex−PCL−HEMA spacer. The weight loss of the DN2 hydrogel in a PBS buffer (without enzyme) was added as the control (DNC). At 37 °C, the degradation of the DN hydrogels was faster during the first 3 days. The weight loss of the hydrogels in the first day varied from 2.8% to 10.9%, as shown in Figure 7. The DN1 hydrogel reached a stable stage after 3 days, and the weight losses of the DN2, DN3, and DN4 hydrogels increased slightly within the time range from 4 to 16 days. During the

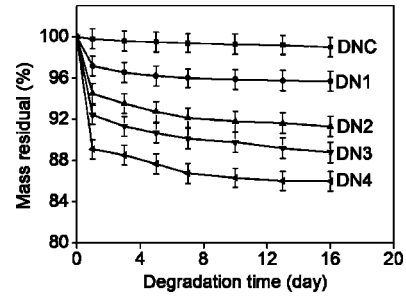

FIGURE 7. Weight loss of the Dex−PCL−HEMA/PNIPAAm hydrogels under the enzyme lipase from *P. cepacia* in a PBS solvent (pH 7.4) at 37 °C.

first 3 days, owing to the fact that the Dex chain was exposed in the buffer solution, hydrolysis of the ester bonds between Dex and PCL−HEMA occurred. Because of the rupture of cross-links in the hydrogels, the Dex chains linked with the degraded cross-links were released and diffused into the buffer solutions. Because Dex chains were hydrophilic and PNIPAAm chains were hydrophobic at 37 °C, with more freed Dex diffusing from the hydrogel, the remaining hydrogel networks became more hydrophobic. Thus, water diffusion and access to the polymer chain got more difficult. As presented in Figure 7, the weight loss of DN2, DN3, and DN4 increased after 3 days, and the reason is probably that, with the lipase from a *P. cepacia* solution immersing into the hydrophobic moieties, the PCL chain broke down and diffused into the buffer solution. At the end of 16 days, the PCL chain became almost degraded and the weight loss reached a stable stage. With an increase in the content of the

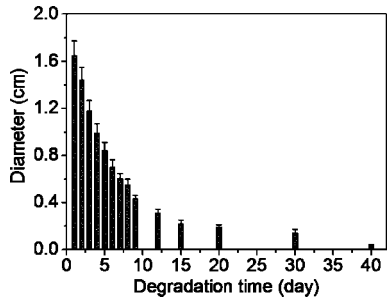

FIGURE 8. In vivo degradation of the injected Dex−PCL−HEMA/PNIPAAm hydrogel (DN2), showing the transverse diameter as a function of the time. The hydrogel was injected SC beneath the dorsal skin between the scapulae.

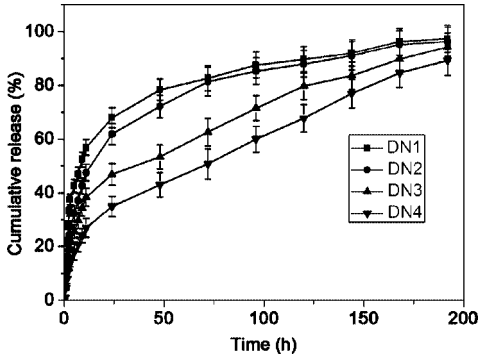

FIGURE 9. Cumulative amounts of BSA released from the Dex−PCL−HEMA/PNIPAAm hydrogels at 37 °C.

hydrophilic Dex chain, the degradation rates and weight loss rates of the DN hydrogels were DN1 < DN2 < DN3 < DN4.

In Vivo Degradation of the Hydrogels. SC injection of the hydrogel into rats is shown in Figure 8. The hydrogel rendered a gel state after injection as observed and the hydrogel became stiff. As shown in Figure 8, the transverse diameter of the hydrogel after injection under the dorsal skin between the scapulae decreased as time passed. It decreased drastically during the first week and was about half as large as the initial diameter of the injection at the end of this week. The diameter of the hydrogel became steady after 2 weeks, and the value was about one-fourth of the initial injection. Compared to the in vitro degradation in a PBS solution, the degree of in vivo degradation is much larger. The molecular weight of the PNIPPAm chain piece after degradation of the cross-linker Dex−PCL−HEMA was not more than 10 000 g/mol, which allowed the low molecular weight PNIPAAm chains to filter through the kidney membrane (48).

In Vitro Release of BSA from the Hydrogels. The cumulative amounts of BSA released from the DN hydrogels at 37 °C are shown in Figure 9. The release profiles exhibited a fast release rate in the initial 5 h; the cumulative BSA releases were 39%, 30%, 23%, and 17% for DN1, DN2, DN3, and DN4, respectively. Because degradation of the cross-linker was faster during the first day, the hydrophilic model drug BSA diffused quickly into the buffer solution. However, release of BSA became a virtually constant zero-order rate over a 7-day period. With degradation of the ester bonds of the cross-liker, the hydrophilic Dex chains diffused into the buffer solution, and hydrogels became more and more hydrophobic. Also the collapsed PNIPAAm hydrogel

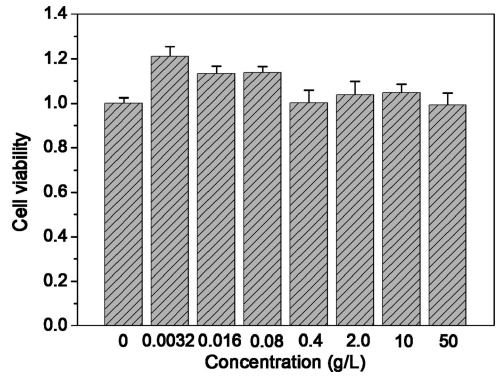

FIGURE 10. Cytotoxicity studies of the Dex−PCL−HEMA/PNIPAAm hydrogel with different concentrations.

network at 37 °C may greatly entrap the residual BSA in the collapsed matrix and thereafter postpone BSA release for a longer period (49). When the degradation rate of the DN hydrogels came to a moderate stage, the released BSA amounts increased in a linear relationship as a function of the time. At the end of degradation of the DN hydrogels, the release behavior came to an end. Therefore, it is inferred that the release of the macromolecular model drug BSA was controlled mainly by the dissolution and dissociation of the DN hydrogels, rather than by a diffusion mechanism.

Cytotoxicity Study of the Hydrogels. MTT assay was performed to investigate the cytotoxcity of the hydrogels. The effect of the hydrogel concentration on the proliferation of ECV304 was studied (Figure 10). The results demonstrate that there is a nonsignificant decrease in the cell viability when the concentration of the hydrogel is between 0.0032 and 50 g/L. It is obvious that the hydrogel has no apparent cytotoxicity.

In Vivo Biocompatibility of the Hydrogels. During the in vivo experiment period, neither reduction of the locomotor activity of all rats' hind limbs nor a change of the food intake was found. Regional cutaneous necrosis around the injection site was found in one rat of group 2, which was relieved by applying erythromycin ointment for 4 days; no red swelling of the skin or necrosis was detected in the rest of the rats. As shown in Figure 11B, The frozen section of implants showed a slight inflammatory response. Because of biodegradation of the DN2 hydrogel in the tissues, there is a need to investigate the function of the liver and kidney and blood indicators after injection of the DN2 hydrogel. Figure 12 demonstrates the concentrations of blood cells, blood glucose, AST, ALT, BUN, and Cr. After 1 week of injection, the concentrations of the control, IM and SC groups are listed as follows. (A) White blood cell: 6.7222, 7.4500, and 8.3930×10^9 cells/L; $P = 0.289$. Red blood cell: 5.8000, 6.6620, and 6.6740×10^{12} cells/L; $P = 0.125$. Lymphocyte: 5.9889, 6.1300, and 6.9210×10^9 cells/L; $P = 0.152$. Platelet: 699.222, 726.5000, and 739.000×10^9 cells/L; $P = 0.060$. (B) Blood glucose: 7.6022, 7.3510, and 7.6030 mmol/L; $P = 0.122$. (C) Aspartate aminotransferase: 51.2556, 51.700, and 45.5700 U/L; $P = 0.939$. Alanine aminotransferase: 152.1889, 145.8500, and 157.8400 U/L; $P = 0.061$. (D) Blood urea nitrogen: 6.2767, 5.8960, and 6.0240 U/L; P

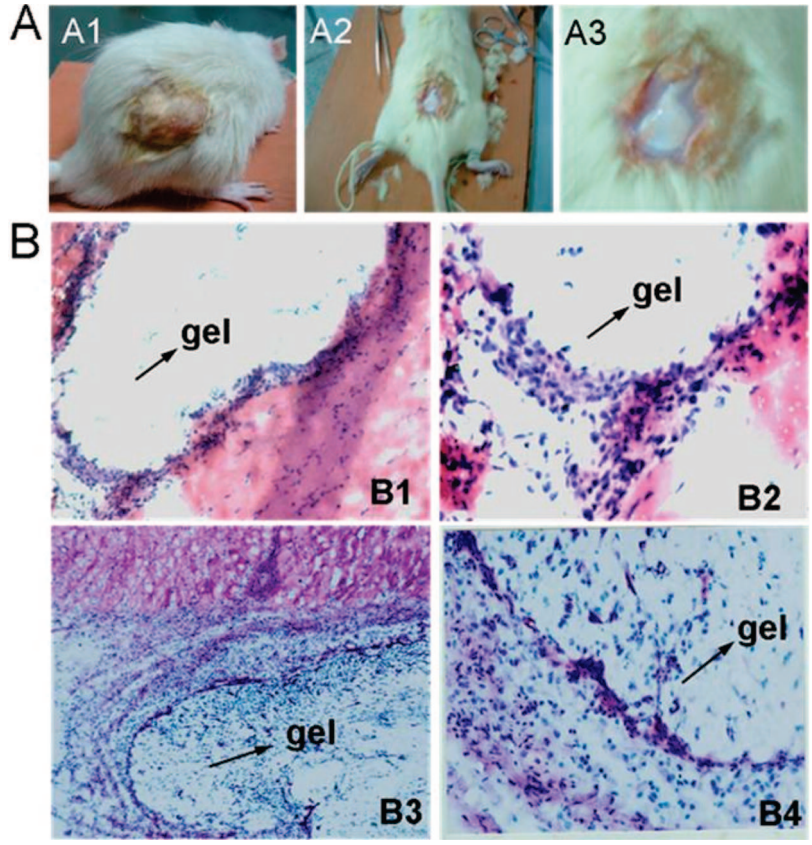

FIGURE 11. (A) Injection of the Dex−PCL−HEMA/PNIPAAm hydrogels. A1: injection site in the rat. A2: natural state of the hydrogel after injection instantly. A3: amplificatory injection site of A2. (B) Sections of implants with surrounding tissues after 1 week of injection of the Dex−PCL−HEMA/PNIPAAm hydrogels (arrows indicate the injected hydrogel). B1: IM injection (40×). B2: IM injection (200×). B3: SC injection (40×). B4: SC injection (200×). All of the sections were stained with HES.

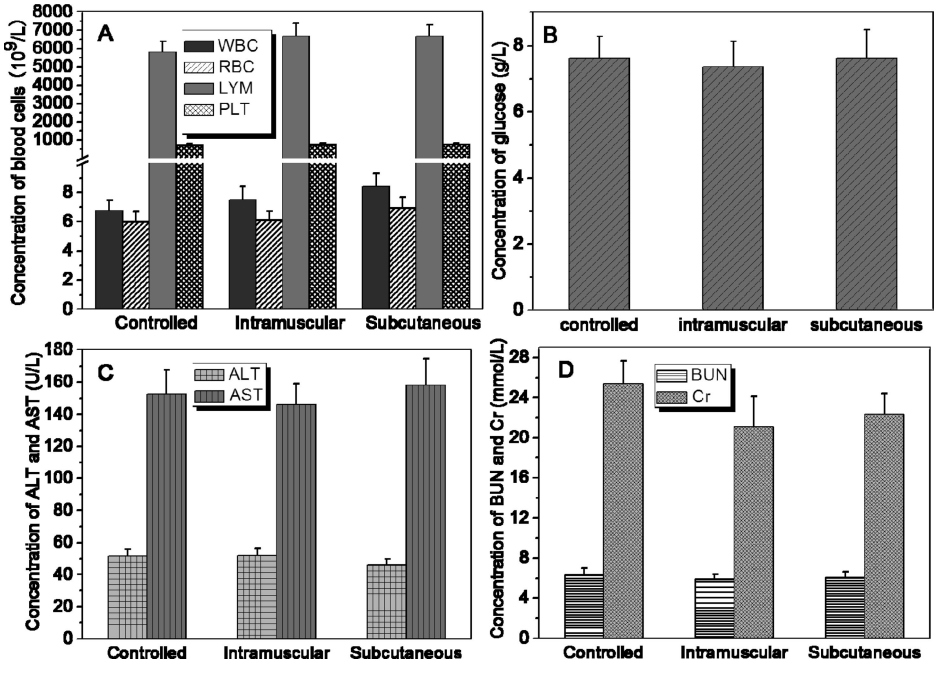

FIGURE 12. Comparison of the biochemical indicators of the three groups (control, IM, and SC) of rats after injection with the Dex−PCL−HEMA/PNIPAAm hydrogels after 1 week: (A) white blood cell (WBC; $P = 0.289$), red blood cell (RBC; $P = 0.125$), lymphocyte (LYM; $P = 0.152$), platelet (PLT; $P = 0.060$); (B) blood glucose ($P = 0.122$); (C) aspartate aminotransferase (AST; $P = 0.939$), alanine aminotransferase (ALT; $P = 0.061$); (D) blood urea nitrogen (BUN; $P = 0.992$), creatinine (Cr; $P = 0.080$). $P < 0.05$ indicates that there is statistical significance among the groups. In this study, all $P > 0.05$, which means that there is no statistical significance among the groups.

= 0.992. Creatinine: 152.1889, 145.8500, and 157.8400 U/L; $P = 0.080$. Seen from the P values mentioned above, all of them are more than 0.05, which indicates that there is no statistical significance among the groups. The hydrogel showed excellent biocompatibility in our investigation because of degradation of the polymer Dex−PCL−HEMA, which could be degraded by enzymes in vivo, and the PCL chain could be licked up by macrophage.

CONCLUSIONS

Dex−PCL−HEMA/PNIPAAm hydrogels were synthesized and characterized in vitro and in vivo. The hydrogels exhibited a phase transition temperature at 33.2 °C, which was suitable for injection through a small-diameter aperture. The sustained release of BSA from the hydrogel was observed when the temperature was higher than the LCST of the hydrogel. Cell viability studies in vitro and histological studies in vivo demonstrated that the hydrogel was a promising candidate of an injectable polymer scaffold for tissue engineering applications. The study of a hydrogel scaffold for stem cell encapsulation is currently in progress in our laboratory.

Acknowledgment. This work was supported by the National Natural Science Foundation of China (Grants 20774069 and 50633020), National Key Basic Research Program of China (Grant 2005CB623903), and Ministry of Education of China (Cultivation Fund of Key Scientific and Technical Innovation Project 707043).

REFERENCES AND NOTES

(1) Bae, Y. H.; Kim, S. W. *Adv. Drug Delivery Rev.* **1993**, *11*, 109–135.
(2) Peppas, N. A.; Sahlin, J. J. *Biomaterials* **1996**, *17*, 1553–1561.
(3) Chen, G.; Imanishi, Y.; Ito, Y. *Langmuir* **1998**, *14*, 6610–6612.
(4) Torres-Lugo, M.; Peppas, N. A. *Macromolecules* **1999**, *32*, 6646–6651.
(5) Wu, D. Q.; Sun, Y. X.; Xu, X. D.; Cheng, S. X.; Zhang, X. Z.; Zhuo, R. X. *Biomacromolecules* **2008**, *9*, 1155–1162.
(6) Hoffman, A. S. *J. Controlled Release* **1987**, *6*, 297–305.
(7) Zhang, X. Z.; Yang, Y. Y.; Wang, F. J.; Chung, T. S. *Langmuir* **2002**, *18*, 2013–2018.
(8) Park, J. S.; Akiyama, Y.; Winnik, F. M.; Kataoka, K. *Macromolecules* **2004**, *37*, 6786–6792.
(9) Miyata, T.; Asami, N.; Uragami, T. *Nature* **1999**, *399*, 766–769.
(10) Li, H.; Chen, J.; Lam, K. Y. *Biomacromolecules* **2006**, *7*, 1951–1959.
(11) Stayton, P. S.; Shimoboji, T.; Long, C.; Chilkoti, A.; Chen, G.; Harris, J. M.; Hoffman, A. S. *Nature* **1995**, *378*, 472–474.
(12) Taguchi, T.; Xu, L. M.; Kobayashi, H.; Taniguchi, A.; Kataoka, K.; Tanaka, J. *Biomaterials* **2005**, *26*, 1247–1252.
(13) Jackson, J. K.; Liang, L. S.; Hunter, W. L.; Reynolds, M.; Sandberg, J. A.; Springate, C.; Burt, H. M. *Int. J. Pharm.* **2002**, *243*, 43–55.
(14) Temenoff, J. S.; Park, H.; Jabbari, E.; Conway, D. E.; Sheffield, T. L.; Ambrose, C. G.; Mikos, A. G. *Biomacromolecules* **2004**, *5*, 5–10.
(15) Jeong, B.; Bae, Y. H.; Kim, S. W. *J. Controlled Release* **2000**, *63*, 155–163.
(16) Westhaus, E.; Messersmith, P. B. *Biomaterials* **2001**, *22*, 453–462.
(17) Park, H.; Temenoff, J. S.; Holland, T. A.; Tabata, Y.; Mikos, A. G. *Biomaterials* **2005**, *26*, 7095–7103.
(18) Van Tomme, S. R.; van Nostrum, C. F.; de Smedt, S. C.; Hennink, W. E. *Biomaterials* **2006**, *27*, 4141–4148.
(19) Qiao, M. X.; Chen, D. W.; Ma, X. C.; Liu, Y. J. *Int. J. Pharm.* **2005**, *294*, 103–112.
(20) Stile, R. A.; Burghardt, W. R.; Healy, K. E. *Macromolecules* **1999**, *32*, 7370–7379.
(21) Ho, E.; Lowman, A.; Marcolongo, M. *Biomacromolecules* **2006**, *7*, 3223–3228.
(22) Holland, T. A.; Mikos, A. G. *J. Controlled Release* **2003**, *86*, 1–14.
(23) Hwang, M. J.; Suh, J. M.; Bae, Y. H.; Kim, S. W.; Jeong, B. *Biomacromolecules* **2005**, *6*, 885–890.
(24) Bae, S. J.; Suh, J. M.; Sohn, Y. S.; Bae, Y.; Kim, S. W.; Jeong, B. *Macromolecules* **2005**, *38*, 5260–5265.
(25) Hoffman, A. S. *MRS Bull.* **1991**, *16*, 42–46.
(26) Gil, E. S.; Hudson, S. M. *Prog. Polym. Sci.* **2004**, *29*, 1173–1222.
(27) Tsuda, Y.; Kikuchi, A.; Yamato, M.; Sakurai, Y.; Umezu, M.; Okano, T. *J. Biomed. Mater. Res.* **2004**, *69A*, 70–78.
(28) Liu, Y.; Lu, W. L.; Wang, J. C.; Zhang, X.; Zhang, H.; Wang, X. Q.; Zhou, T. Y.; Zhang, Q. *J. Controlled Release* **2007**, *117*, 387–395.
(29) Dong, J.; Chen, L.; Ding, Y. M.; Han, W. J. *Macromol. Chem. Phys.* **2005**, *206*, 1973–1980.
(30) Ouchi, T.; Kontani, T.; Aoki, R.; Saito, T.; Ohya, Y. *J. Polym. Sci., Part A: Polym. Chem.* **2006**, *44*, 6402–6409.
(31) Graham, D. L.; Ferreira, H.; Bernardo, J.; Freitas, P. P.; Cabral, J. M. S. *J. Appl. Phys.* **2002**, *91*, 7786–7788.
(32) Izutsu, K. I.; Aoyagi, N.; Kojima, S. *J. Pharm. Sci.* **2005**, *94*, 709–717.
(33) Rhee, S. H.; Choi, J. Y.; Kim, H. M. *Biomaterials* **2002**, *23*, 4915–4921.
(34) Kweon, H. Y.; Yoo, M. K.; Park, I. K.; Kim, T. H.; Lee, H. C.; Lee, H. S.; Oh, J. S.; Akaike, T.; Cho, C. S. *Biomaterials* **2003**, *24*, 801–808.
(35) Prabu, P.; Dharmaraj, N.; Aryal, S.; Lee, B. M.; Ramesh, V.; Kim, H. Y. *J. Biomed. Mater. Res., Part A* **2006**, *79A*, 153–158.
(36) Gilbert, R. D.; Stannett, V.; Pitt, C. G.; Schindler, A. In *The Design of Biodegradable Polymers: Two Approaches in Development in Polyme Degradation*; Grassie, N., Ed.; Elsevier: Amsterdam, The Netherlands, 1982; pp 259−293.
(37) de Jong, S. J.; De Smedt, S. C.; Wahls, M. W. C.; Demeester, J.; Kettenes-van den Bosch, J. J.; Hennink, W. E. *Macromolecules* **2000**, *33*, 3680–3686.
(38) Hellio-Serughetti, D.; Djabourov, M. *Langmuir* **2006**, *22*, 8516–8522.
(39) Menger, F. M; Caran, K. L. *J. Am. Chem. Soc.* **2000**, *122*, 11679–11691.
(40) Vemula, P. K.; John, G. *Chem. Commun.* **2006**, *21*, 2218–2220.
(41) Jarry, C.; Chaput, C.; Chenite, A.; Renaud, M. A.; Buschmann, M.; Leroux, J. C. *J. Biomed. Mater. Res., Part B* **2001**, *58*, 127–135.
(42) Hirotsu, S.; Hirokawa, Y.; Tanaka, T. *J. Chem. Phys.* **1987**, *87*, 1392–1395.
(43) Ebara, M.; Aoyagi, T.; Sakai, K.; Okano, T. *Macromolecules* **2000**, *33*, 8312–8316.
(44) Zhang, J.; Peppas, N. A. *Macromolecules* **2000**, *33*, 102–107.
(45) Kobayashi, S.; Uyama, H.; Takamoto, T. *Biomacromolecules* **2000**, *1*, 3–5.
(46) Kumashiro, Y.; Ooya, T.; Yui, N. *Macromol. Rapid Commun.* **2004**, *25*, 867–872.
(47) Kumashiro, Y.; Lee, W. K.; Ooya, T.; Yui, N. *Macromol. Rapid Commun.* **2002**, *23*, 407–410.
(48) Jeong, B.; Bae, Y. H.; Lee, D. S.; Kim, S. W. *Nature* **1997**, *388*, 860–862.
(49) Zhang, X. Z.; Wu, D. Q.; Chu, C. C. *Biomaterials* **2004**, *25*, 3793–3805.

AM8000456